THE JOURNAL OF BIOLOGICAL CHEMISTRY VOL. 285, NO. 46, pp. 35988–35998, November 12, 2010

$BcsK_C$ Is an Essential Protein for the Type VI Secretion System Activity in *Burkholderia cenocepacia* That Forms an Outer Membrane Complex with $BcsL_B$*[S]

Received for publication, March 5, 2010, and in revised form, August 15, 2010 Published, JBC Papers in Press, August 20, 2010, DOI 10.1074/jbc.M110.120402

Daniel Aubert[‡1], **Douglas K. MacDonald**[‡], **and Miguel A. Valvano**[‡§2]

From the Departments of [‡]*Microbiology and Immunology and* [§]*Medicine, Infectious Diseases Research Group, Siebens Drake Medical Research Institute, University of Western Ontario, London, Ontario N6A 5C1, Canada*

The type VI secretion system (T6SS) contributes to the virulence of *Burkholderia cenocepacia*, an opportunistic pathogen causing serious chronic infections in patients with cystic fibrosis. $BcsK_C$ is a highly conserved protein among the T6SSs in Gram-negative bacteria. Here, we show that $BcsK_C$ is required for Hcp secretion and cytoskeletal redistribution in macrophages upon bacterial infection. These two phenotypes are associated with a functional T6SS in *B. cenocepacia*. Experiments employing a bacterial two-hybrid system and pulldown assays demonstrated that $BcsK_C$ interacts with $BcsL_B$, another conserved T6SS component. Internal deletions within $BcsK_C$ revealed that its N-terminal domain is necessary and sufficient for interaction with $BcsL_B$. Fractionation experiments showed that $BcsK_C$ can be in the cytosol or tightly associated with the outer membrane and that $BcsK_C$ and $BcsL_B$ form a high molecular weight complex anchored to the outer membrane that requires $BcsF_H$ (a ClpV homolog) to be assembled. Together, our data show that $BcsK_C$/$BcsL_B$ interaction is essential for the T6SS activity in *B. cenocepacia*.

The *Burkholderia cepacia* complex comprises closely related species of Gram-negative bacteria commonly found in the environment (1, 2). *B. cepacia* complex bacteria are opportunistic human pathogens that establish chronic lung infections in immunocompromised patients with chronic granulomatous disease or, most commonly, cystic fibrosis (3). In most cystic fibrosis centers worldwide and more particularly in Canada, *Burkholderia cenocepacia* is one of the most common *B. cepacia* complex species recovered from patients (4, 5) and is frequently associated with the most severe infections (6).

Novel factors for *B. cenocepacia* survival *in vivo* were discovered in our laboratory by signature-tagged mutagenesis using a rat model of chronic lung infection (7), and these included a type 6 secretion system (T6SS)[3] (7, 8). The T6SS is a newly recognized secretion system widespread among Gram-negative pathogens and symbionts that are in close interaction with eukaryotic cells (9–11). Several proteins specifically secreted by the T6SS into culture supernatants have been identified. These proteins usually lack any conventional N-terminal hydrophobic signal peptide and include the hemolysin coregulated-like protein (Hcp) (12), the valine-glycine repeat family proteins (VgrG) (13), and in some cases non-Hcp, non-VgrG substrates (12, 14, 15). Hcp is secreted by most of the T6SSs studied to date, and its detection in culture supernatants is considered the hallmark of a functional T6SS (8, 16–19). Hcp and VgrG proteins might also be part of the T6SS structural scaffold displayed at the bacterial surface and might be released into culture supernatants by shearing forces (20, 21).

The T6SS contributes to the pathogenicity of many bacteria (12, 16, 17, 22, 23). In *Vibrio cholerae*, bacteria-host contact and endocytosis are required to trigger the translocation of VgrG-1 into the host cell cytosol. Cytosolic VgrG-1 mediates actin cross-linking impairing the phagocytic cell functions (24). Although in some bacteria the T6SS has evolved to target eukaryotic cells, the *Pseudomonas aeruginosa* T6SS has been recently shown to deliver toxins into other bacteria. This novel T6SS property would confer a fitness advantage to *P. aeruginosa* growing in bacterial communities (25).

Typically, the T6SS is poorly expressed under *in vitro* laboratory conditions, but it is quorum sensing regulated (19, 26) and induced *in vivo* during infection (9, 11, 27). We have recently identified AtsR, a sensor kinase-response regulator hybrid that negatively regulates the T6SS expression in *B. cenocepacia* K56-2 (8). Deletion of *atsR* causes increased T6SS activity, as exemplified by hypersecretion of Hcp into culture supernatant (8). Infection of macrophages with the *atsR* deletion strain induces cytoskeletal rearrangements, resulting in macrophages displaying actin-rich cellular projections (8). This phenotype relies on T6SS activity and has only been described for *B. cenocepacia*, but the *B. cenocepacia* effector molecules and the eukaryotic targets involved in this process are unknown and currently under investigation in our laboratory.

Similarity between bacteriophage proteins and the T6S-associated Hcp and VgrG proteins suggests that the T6SS is structurally and evolutionarily related to bacteriophages (21, 28). Several components highly conserved among T6SSs have been

* This work was supported by a grant from the Canadian Cystic Fibrosis Foundation (to M. A. V.).

[S] The on-line version of this article (available at http://www.jbc.org) contains supplemental text, Tables S1 and S2, and Figs. S1–S4.

[1] Supported by a postdoctoral fellowship from the Canadian Institutes of Health Research in partnership with the Association of Medical Microbiology and Infectious Disease Canada.

[2] Canada Research Chair in Infectious Diseases and Microbial Pathogenesis. Recipient of a Senior Researcher Training Award from the Canadian Cystic Fibrosis Foundation. To whom correspondence should be addressed: Dept. of Microbiology and Immunology, Dental Sciences Bldg. 3014, University of Western Ontario, London, Ontario N6A 5C1, Canada. Tel.: 519-661-3427; Fax: 519-661-3499; E-mail: mvalvano@uwo.ca.

[3] The abbreviation used is: T6SS, type VI secretion system.

investigated, and some light has been shed on their localization, function, and interaction with other T6SS components. These include: (i) the integral inner membrane IcmF-like protein (ImpL$_M$) from *Agrobacterium tumefaciens* (29); (ii) the outer membrane lipoprotein SciN (30); (iii) the polytopic inner membrane protein SciZ anchoring the T6SS to the cell wall (31) in enteroaggregative *Escherichia coli*; (iv) the proteins VipA in *V. cholerae* (32) and its homolog IglA in *Francisella novicida*, which interact with VipB and IglB (11), respectively; and (v) the energizing component ClpV, which disintegrates cytosolic tubule like structures made of VipA and VipB (32).

This study focuses on BcsK$_C$, a T6SS component from *B. cenocepacia* homologous to IglB. We show here that BcsK$_C$ is critical for the T6SS activity of *B. cenocepacia* K56-2. Experiments employing the bacterial two-hybrid system confirmed that BcsK$_C$ also interacts with BcsL$_B$, a protein homologous to IglA, and support the notion that interactions between BcsL$_B$- and BcsK$_C$-like proteins are a common feature of T6SSs. Internal deletions of BcsK$_C$ allowed us to characterize the region required for BcsL$_B$ binding and demonstrated that the N terminus of BcsK$_C$ is essential and sufficient for interaction with BcsL$_B$. Furthermore, cell fractionation experiments revealed that BcsK$_C$ can be tightly associated with the outer membrane and that BcsK$_C$, in association with BcsL$_B$, forms a membrane associated high molecular weight complex whose assembly requires BcsF$_H$ (ClpV homolog). Together, this work establishes BcsK$_C$ as a critical component of the T6S apparatus.

EXPERIMENTAL PROCEDURES

Bacterial Strains, Plasmids, and Culture Media—Bacterial strains and plasmids used in this study are listed in supplemental Table S1. Bacteria were routinely cultured in LB (Difco) at 37 °C. *E. coli* cultures were supplemented, as required, with the following antibiotics (final concentrations): 100 μg/ml ampicillin, 30 μg/ml tetracycline, 30 μg/ml kanamycin, 30 μg/ml chloramphenicol, 50 μg/ml trimethoprim, and 50 μg/ml gentamicin. *B. cenocepacia* cultures were supplemented, as required, with 100 μg/ml trimethoprim, 100 μg/ml tetracycline, and 50 μg/ml gentamicin. We used the unified nomenclature proposed by Cascales (33) and assigned the alphabetical character designated by Shalom *et al.* (34) to the T6SS genes from *B. cenocepacia* K56-2.

General Molecular Techniques—DNA manipulations were performed as described previously (35). T4 polynucleotide kinase and T4 DNA ligase (Roche Applied Science) were used as recommended by the manufacturers. Transformation of *E. coli* DH5α, *E. coli* SY327, and *E. coli* KEM5 was done by the calcium chloride protocol (36). Mobilization of complementing plasmids and mutagenesis plasmids into *B. cenocepacia* K56-2 was performed by triparental mating using *E. coli* DH5α carrying the helper plasmid pRK2013 (37, 38). DNA amplification by PCR was performed using a PTC-221 DNA engine (MJ Research, Incline Village, Nevada) with *Taq*, Proof Start, or HotStar HiFidelity DNA polymerases (Qiagen). DNA sequences of all of the primers used in this study are described in supplemental Table S2. DNA sequencing was performed at the DNA sequencing facility of York University (Toronto, Canada). The computer program BLAST was used to analyze the sequenced genome of *B. cenocepacia* strain J2315.

Mutagenesis of B. cenocepacia K56-2 and Complementing Plasmids—Unmarked and nonpolar deletions were performed as described previously (39). Details about the construction of the deletion plasmids are available in the supplemental materials. Plasmid pDelatsR was used to delete *atsR* (*BCAM0379*) in *B. cenocepacia* K56-2. Deletions were subsequently performed in the *atsR*-deleted mutant, *B. cenocepacia* K56-2 Δ*atsR*. Plasmids pDelT6SS, pDelTU1, pDelTU2, and pDelTU3 were used to delete the entire T6SS gene cluster: T6SS transcriptional units 1, 2, and 3, respectively. Each gene within transcriptional unit 2 was individually deleted. Plasmids pDelbcsM, pDelbcsL$_B$, pDelbcsK$_C$, pDA45, pDelbcsI$_E$, pDelbcsH$_F$, pDelbcsG$_G$, pDelbcsF$_H$, and pDelbcsE$_A$ were used to delete *BCAL0340*, *0341*, *0342*, *0343*, *0344*, *0345*, *0346*, *0347*, and *BCAL0348*, respectively. Gene deletions were first analyzed by PCR and also confirmed by Southern blot hybridization.

The *bcsK$_C$* gene was PCR-amplified using primer pair 3401–3393. Amplicons were digested with the restriction enzymes KpnI-SacI and cloned into a similarly digested pME6000 plasmid, giving rise to pBcsK$_C$. We took advantage of two SphI restriction sites within the *bcsK$_C$* gene sequence to generate an in-frame deletion of 0.45 kb. The *bcsK$_C$* gene was PCR-amplified as described above and digested with KpnI, SacI, and SphI, generating three fragments (0.13, 0.45, and 0.93 kb). Only the 0.13- and 0.93-kb fragments were gel-purified using the QiaQuick gel extraction kit (Qiagen) and cloned as above into the KpnI-SacI-digested pME6000 plasmid, giving rise to pBcsK$_{CΔ40–189}$.

A FLAG epitope was fused to the N termini of BcsK$_C$ and BcsK$_{CΔ40–189}$ as follows. The *bcsK$_C$* and *bcsK$_{CΔ40–189}$* genes were PCR-amplified using primer pair 3700–3701. Amplicons were digested with the restriction enzymes HindIII-BamHI and cloned into a similarly digested pEL-1 plasmid giving rise to pBcsK$_{C\text{-}FLAG}$ and pBcsK$_{CΔ40–189\text{-}FLAG}$.

Preparation of Culture Supernatant Proteins—Culture supernatant proteins were precipitated with trichloroacetic acid as described previously (8). Ten μg of protein were loaded on a 16% SDS-PAGE. Detection was performed with a Brilliant Blue G colloidal staining according to the manufacturer's recommendations (Sigma).

Pulldown Assay and MS—Protein G-agarose beads (Roche Applied Science; 20-μl packed volume/sample) were washed three times with 20 volumes of TBS. Five μg of FLAG M2 monoclonal antibody (Sigma) per sample were incubated with the bead suspensions with constant agitation for 2 h at 4 °C using a Barnstead Thermolyne LABQUAKE (Barnstead International, Dubuque, IA). The beads were washed three times with 20 volumes of TBS. Overnight cultures of *B. cenocepacia* K56-2 mutants Δ*atsR* Δ*bcsK$_C$* (pEL-1), Δ*atsR* Δ*bcsK$_C$* (pBcsK$_{C\text{-}FLAG}$), and Δ*atsR* Δ*bcsK$_C$* (pBcsK$_{CΔ40–189\text{-}FLAG}$) were 10-fold diluted in 50 ml of prewarmed LB. After 3 h of incubation at 37 °C, the cultures were centrifuged for 10 min at 10,000 × *g* at 4 °C. Bacterial pellets were washed twice with 10 ml of TBS and resuspended in 4 ml of TBS containing a protease inhibitor mixture (Roche Applied Science). The cells were lysed by three passages in a French press (Thermo

Scientific) using a miniature French pressure cell at 600 p.s.i. The cell lysates were centrifuged first at 5000 × *g* at 4 °C for 15 min, and the supernatants were transferred in fresh tubes, centrifuged at 21,000 × *g* for 15 min, and collected. The bead suspensions conjugated to the FLAG antibody were added to 1 ml of each supernatant and incubated for 3 h at 4 °C with constant rotation. The beads were washed three times with 10 volumes of TBS and resuspended in 100 μl of TBS. Twenty μl of bead suspension were boiled and loaded in duplicate on a 16% SDS-PAGE gel. After electrophoresis, detection was performed on half of the gel by silver staining adapted from Blum *et al.* (40). The other half of the gel was transferred to a nitrocellulose membrane for immunoblot analysis (see below).

Protein bands were excised from a silver-stained one-dimensional gel using an Ettan Spot-Picker (Amersham Biosciences). In-gel trypsin digestion was performed in the Functional Proteomics Facility of the University of Western Ontario using the Waters MassPREP automated station. Five μl of submitted sample was injected for LC/MS/MS analysis as described elsewhere (8). The data were processed using the Proteinlynx Global Server software, and a database search was performed using MASCOT search engine (Matrix Science, London, UK). This search also provides a score estimating the probability that the observed match between experimental data and each protein in the database is a random event. The higher the protein score, the higher the confidence that the protein in the sample corresponds to the match.

Bacterial Two-hybrid System, β-Galactosidase Assay, and Plasmid Constructions—In vivo interaction between BcsK$_C$ and BcsL$_B$ was investigated using a bacterial adenylate cyclase two-hybrid system kit (Euromedex). This system is based on the interaction-mediated reconstitution of the adenylate cyclase activity in an adenylate cyclase-deficient *E. coli* reporter strain (41). The catalytic domain of adenylate cyclase (CyaA) from *Bordetella pertussis* consists of two complementary fragments, T25 and T18, that are not active when physically separated. When these two fragments are fused to interacting polypeptides and coexpressed in *E. coli*, heterodimerization of the hybrid proteins restores the activity CyaA, leading to cyclic AMP synthesis and transcriptional activation of the *lac* operon. Therefore, interaction between two hybrid proteins in *E. coli* will generate high levels of β-galactosidase activity, which can be readily scored on X-gal-containing medium and quantified.

BcsL$_B$ and BcsK$_C$ were fused to T25 and T18, respectively (details are available in the supplemental materials). Plasmid pT25BcsL$_B$ encodes a hybrid protein made of BcsL$_B$ fused to the C terminus of the T25 fragment (T25-BcsL$_B$). Plasmids pT18BcsK$_C$ and pT18BcsK$_{CΔ40–189}$ encode hybrid proteins made of BcsK$_C$ or a truncated variant fused to the C-terminal end of T18. Plasmids pBcsK$_C$T18 and pBcsK$_{CΔ40–189}$T18 encode hybrid proteins made of BcsK$_C$ or a truncated variant fused to the N-terminal end of T18.

Sequential 25-amino acid deletions were performed within BcsK$_C$ (details are available in the supplemental materials). Deletion of amino acids 38–62, 63–87, 88–112, 113–137, 138–162, 163–187, 188–212, 213–237, and 213–496 were performed, giving rise to plasmids pBcsK$_{CΔ38–62}$T18, pBcsK$_{CΔ63–87}$T18, pBcsK$_{CΔ88–112}$T18, pBcsK$_{CΔ113–137}$T18, pBcsK$_{CΔ138–162}$T18, pBcsK$_{CΔ163–187}$T18, pBcsK$_{CΔ188–212}$T18, pBcsK$_{CΔ213–237}$T18, and pBcsK$_{CΔ213–496}$T18, respectively, expressing truncated BcsK$_C$ fused to the N terminus of T18.

The *E. coli* KEM5 reporter strain (lacking any endogenous adenylate cyclase activity) harboring pT25BcsL$_B$ was co-transformed with the recombinant plasmids expressing hybrid proteins fused to the T18 domain. Bacterial cultures were grown for 16 h in LB at 30 °C with antibiotics as required and isopropyl β-D-1-thiogalactopyranoside (0.5 mM). Samples were taken to measure the bacterial growth ($A_{600\ nm}$) and the β-galactosidase activity ($A_{420\ nm}$ and $A_{550\ nm}$) upon lysis and incubation with *O*-nitrophenyl-β-D-galactoside according to Miller (42). Enzyme activities (Miller units) were calculated using the equation $[(A_{420\ nm} - 1.75\,A_{550\ nm}) \times 1000]/[\text{reaction time (min)} \times \text{culture volume (ml)} \times A_{600\ nm}]$. Each sample was analyzed in triplicate during three independent experiments. Four μl of each culture were also spotted on a LB agar plate containing X-gal (40 μg/ml), isopropyl β-D-1-thiogalactopyranoside (0.5 mM), and antibiotics as required. Incubation was performed for 24 and 48 h at 30 and 37 °C.

Cell Fractionation, Sucrose Density Gradient, and Western Blot Analysis—Overnight cultures were diluted in prewarmed LB. After 3 h of incubation at 37 °C, the cultures were centrifuged for 10 min at 10,000 × *g* at 4 °C. Bacterial pellets were washed with 50 mM Tris-HCl, pH 7.4, and resuspended in 5 ml of the same buffer containing a protease inhibitor mixture, PMSF (1 mM), DNase (50 μg/ml), and RNase (50 μg/ml). The cells were lysed by three passages in a French press at 600 p.s.i. Unbroken cells were removed by centrifugation twice at 20,000 × *g* for 15 min at 4 °C. An aliquot of the supernatant corresponding to the total cell lysate was stored at −20 °C, and the remainder was processed to separate the soluble fraction from the total membrane fraction as follows. The membranes were pelleted by ultracentrifugation at 150,000 × *g* for 1 h at 4 °C in a Beckman 70Ti rotor. An aliquot of the supernatant corresponding to the soluble fraction was stored at −20 °C. To increase the purity of the membrane preparation, the pellet was resuspended in 2 ml of 50 mM Tris-HCl, pH 7.4, containing 10% (w/w) sucrose, a protease inhibitor mixture, and 1 mM PMSF and loaded on top of a discontinuous sucrose gradient consisting of 4 ml of 15% (w/w) sucrose placed on top of 4 ml of 55% (w/w) sucrose made in 50 mM Tris-HCl, pH 7.4. Ultracentrifugation was performed at 37,000 rpm for 1 h at 4 °C in a Beckman SW41. The membranes were collected using a syringe by puncturing the side of the tube slightly below the membrane ring. An aliquot corresponding to the total membrane fraction was stored at −20 °C.

The protein concentration of each fraction was determined by Bradford assay (Bio-Rad), and 10 μg of protein were loaded on 12% SDS-PAGE gels. Unless indicated, the samples were not boiled prior to loading. After electrophoresis, the gels were transferred to nitrocellulose membranes for immunoblot analysis. The membranes were incubated with the 4RA2 monoclonal antibody (Neoclone) cross-reacting with the *B. cenocepacia* RNA polymerase subunit 1 mM (cytosolic control) and the FLAG M2 monoclonal antibody (Sigma). The Alexa Fluor

680 goat anti-mouse IgG (Molecular Probes) was used as a secondary antibody. Detection was performed using the Odyssey Infrared Imager (LI-COR Biosciences).

Protein solubilization experiments were performed based on the work of Ma *et al.* (29). Briefly, the membrane fractions were incubated with either 50 mM Tris-HCl, pH 7.4 (control), 1 M NaCl, 6 M urea, 3% Triton X-100, 2% *N*-lauroylsarcosine, or 1% SDS in ice for 1 h and centrifuged at 150,000 × *g* for 1 h at 4 °C in a Beckman 100Ti rotor to separate soluble and insoluble fractions. The pellet was resuspended in 50 mM Tris-HCl, pH 7.4, in the same volume as the soluble fraction and analyzed by Western blot.

To increase the separation of the inner and outer membranes, the cells were incubated at room temperature for 15 min in 20% (w/w) sucrose made in 50 mM Tris-HCl, pH 7.4, with protease inhibitor. DNase (50 μg/ml), RNase (50 μg/ml), EDTA (0.5 μM), and lysozyme (0.1 mg/ml) were added prior to cell lysis. The soluble lysate was loaded on top of a discontinuous sucrose gradient consisting of 4 ml of 25% (w/w) sucrose placed on top of 2 ml of 60% (w/w) sucrose made in 50 mM Tris-HCl, pH 7.4, and centrifuged as indicated previously. The sucrose concentration of the purified total membranes was lowered to 30% (w/w) sucrose and loaded on top of a second discontinuous sucrose gradient consisting of 0.6 ml of 60% and 1.16-ml layers of 56, 53, 50, 47, 44, 41, 38, 35, and 32% (w/w) sucrose. The membrane fractionation was performed by ultracentrifugation at 37,000 rpm for 40 h at 4 °C in a Beckman SW41 rotor. The gradient was collected from top to bottom using a syringe by puncturing holes in the tube every 0.3 cm. Protein content was assessed by measuring the absorption at 280 nm, and the quality of the fractionation was assessed by the detection of the outer membrane porin BCAM1931, by measuring the enzymatic activity of the NADH oxidase (inner membrane marker) (43) and the refractive index of each fraction. Ten-μl aliquots of the collected fractions were loaded on a 12% SDS-PAGE gel. After electrophoresis, the gel was transferred to a nitrocellulose membrane for immunoblot analysis or silver-stained. The samples need to be boiled to detect BCAM1931.

Electroelution—Purified total membranes from *B. cenocepacia* K56-2 Δ*atsR* Δ*bcsK$_C$* (pBcsK$_{C\text{-}FLAG}$) and *B. cenocepacia* K56-2 Δ*atsR* Δ*T6SS* (pBcsK$_{C\text{-}FLAG}$) were prepared as above. One mg of total membrane proteins was loaded in several wells and separated by electrophoresis on 12% SDS-PAGE gels. After electrophoresis, a 4-mm-wide band from the top of the separating gel (containing the high molecular weight proteins) was excised from each gel and minced. The proteins were electroeluted in volatile buffer (50 mM NH_4HCO_3, 0.1% SDS) using a model 422 Electro-Eluter (Bio-Rad) and Green Membrane caps (molecular mass cutoff of 3,500 Da) for 6 h at 20 mA. After the elution the volatile buffer was removed using a spin vacuum, leaving concentrated proteins. The pellets were resuspended with 80 μl of volatile buffer, and protein concentration was estimated by measuring absorbance at 280 nm using a NanoDrop ND-1000 spectrophotometer (Thermo Fisher Scientific, Wilmington, DE). Seventy μg of protein were boiled for 10 min and loaded on a 16% SDS-PAGE gel. Protein was detected by silver staining, and selected protein bands were excised and analyzed by mass spectrometry as indicated above.

Macrophage Infection Assay—The C57BL/6 murine bone marrow-derived macrophage cell line ANA-1 (44) was maintained in DMEM with 10% (v/v) FBS and grown at 37 °C in a humidified atmosphere of 95 and 5% CO_2. Bacteria were added to ANA-1 cells at a multiplicity of infection of 50:1 as described previously (8) and incubated for 4 h at 37 °C. The images were digitally processed using the Northern Eclipse version 6.0 imaging analysis software (Empix Imaging, Mississauga, Canada).

RESULTS

BcsK$_C$ Is Essential for T6SS Activity—The *bcsK$_C$* gene (*BCAL0342*) encodes a 496-amino acid protein (~55 kDa). BLASTP analysis revealed that BcsK$_C$ contains a domain of unknown function, DUF877, and belongs to a family of uncharacterized bacterial proteins that are associated with the T6S locus of many Gram-negative bacteria including *Burkholderia mallei* (TssB), *P. aeruginosa* (PA0084), *V. cholerae* (VipB), *Salmonella enterica* serovar Typhimurium (SciI), *Edwardsiella tarda* (EvpB), and *F. novicida* (IglB).

We have previously demonstrated that inactivation of *atsR* in *B. cenocepacia* K56-2 leads to increased T6SS activity, as exemplified by (i) hypersecretion of an Hcp-like protein and (ii) cytoskeletal reorganization with the formation of cellular projections upon infection of ANA-1 murine macrophages (8). Following these two phenotypes we investigated the importance of BcsK$_C$ in the T6SS activity of *B. cenocepacia* K56-2. Analysis of culture supernatants (Fig. 1*A*) revealed that in contrast to K56-2 Δ*atsR*, the K56-2 Δ*atsR* Δ*bcsK$_C$* double mutant was unable to release Hcp, consistent with a secretion defect. Hcp secretion was restored upon introduction of pBcsK$_C$, which constitutively expresses BcsK$_C$ into K56-2 Δ*atsR* Δ*bcsK$_C$* (Fig. 1*A*). Furthermore, more than 60% of ANA-1 macrophages displayed cellular projections upon infection with K56-2 Δ*atsR* (Fig. 1*B*, *upper left panel*), whereas this phenotype was absent in macrophages infected with K56-2 Δ*atsR* Δ*bcsK$_C$*. Introduction of pBcsK$_C$ into K56-2 Δ*atsR* Δ*bcsK$_C$* (Fig. 1*B*, *lower left panel*) restored the ability of these bacteria to mediate cytoskeletal rearrangements in macrophages. Identical results were obtained with pBcsK$_{C\text{-}FLAG}$ (supplemental Fig. S1), indicating that fusion of a FLAG epitope to the N terminus of BcsK$_C$ does not alter the protein function. Together, these results demonstrate that BcsK$_C$ is essential for T6SS function in *B. cenocepacia* K56-2.

The N Terminus of BcsK$_C$ Is Required for T6SS Activity—We took advantage of two conveniently located SphI restriction sites in *bcsK$_C$* to generate a 0.45-kb truncation of the gene, causing an in frame deletion of 150 amino acids within the BcsK$_C$ N terminus (BcsK$_{C\Delta 40-189}$). Plasmid pBcsK$_{C\Delta 40-189}$ could not restore Hcp secretion in K56-2 Δ*atsR* Δ*bcsK$_C$* (Fig. 1*A*). Moreover, ANA-1 macrophages infected with K56-2 Δ*atsR* Δ*bcsK$_C$* (pBcsK$_{C\Delta 40-189}$) or K56-2 Δ*atsR* Δ*bcsK$_C$* (pBcsK$_{C\Delta 40-189\text{-}FLAG}$) did not display the cellular projections typical of T6SS activity (Fig. 1*B*, *lower right panel*, and supplemental Fig. S1). Western blot analysis of bacterial cell lysates prepared from K56-2 Δ*atsR* Δ*bcsK$_C$* (pBcsK$_{C\text{-}FLAG}$) and K56-2 Δ*atsR* Δ*bcsK$_C$* (pBcsK$_{C\Delta 40-189\text{-}FLAG}$) demonstrated that BcsK$_{C\text{-}FLAG}$ and BcsK$_{C\Delta 40-189\text{-}FLAG}$ were similarly expressed (see below). Thus, a lack of complementation by pBcsK$_{C\Delta 40-189\text{-}FLAG}$ was not due to a defect in protein expression. Together, these data indicate

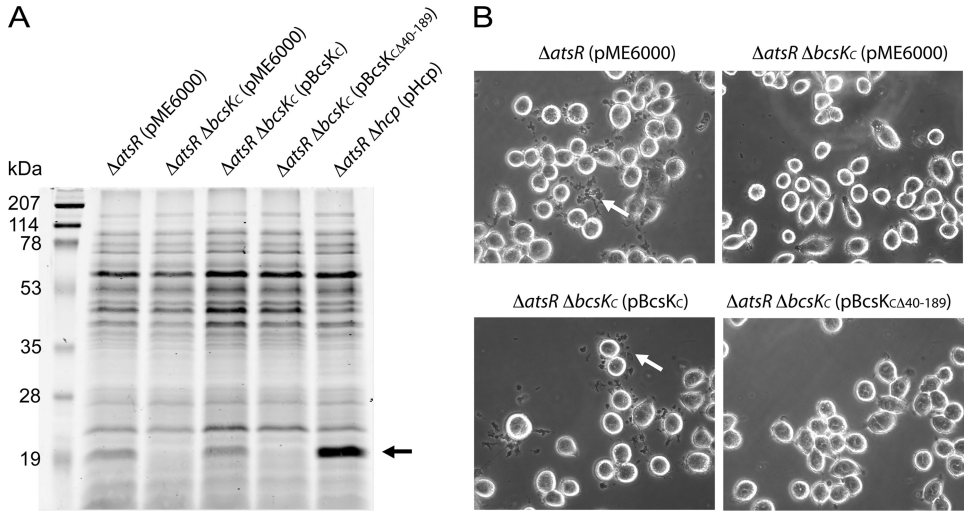

FIGURE 1. **BcsK$_C$ is required for T6SS activity.** *A*, secretion assay. SDS-polyacrylamide gel electrophoresis analysis of concentrated culture supernatants recovered from *B. cenocepacia* K56-2 Δ*atsR* containing the control plasmid pME6000 (Δ*atsR* pME6000), K56-2 Δ*atsR* Δ*bcsK$_C$* (pME6000), K56-2 Δ*atsR* Δ*bcsK$_C$* (pBcsK$_C$), K56-2 Δ*atsR* Δ*bcsK$_C$* (pBcsK$_{CΔ40-189}$), and K56-2 Δ*atsR* Δ*hcp* (pHcp). Shown at *left* is the molecular mass marker with the indicated sizes (kDa). The *black arrow* highlights the position of secreted Hcp. *B*, phase contrast microscopy of infected ANA-1 macrophages. The infections were performed at a multiplicity of infection of 50:1 for 4 h with the following strains: *B. cenocepacia* K56-2 Δ*atsR* (pME6000), K56-2 Δ*atsR* Δ*bcsK$_C$* (pME6000), K56-2 Δ*atsR* Δ*bcsK$_C$* (pBcsK$_C$), and K56-2 Δ*atsR* Δ*bcsK$_C$* (pBcsK$_{CΔ40-189}$). The *white arrows* indicate cellular projections.

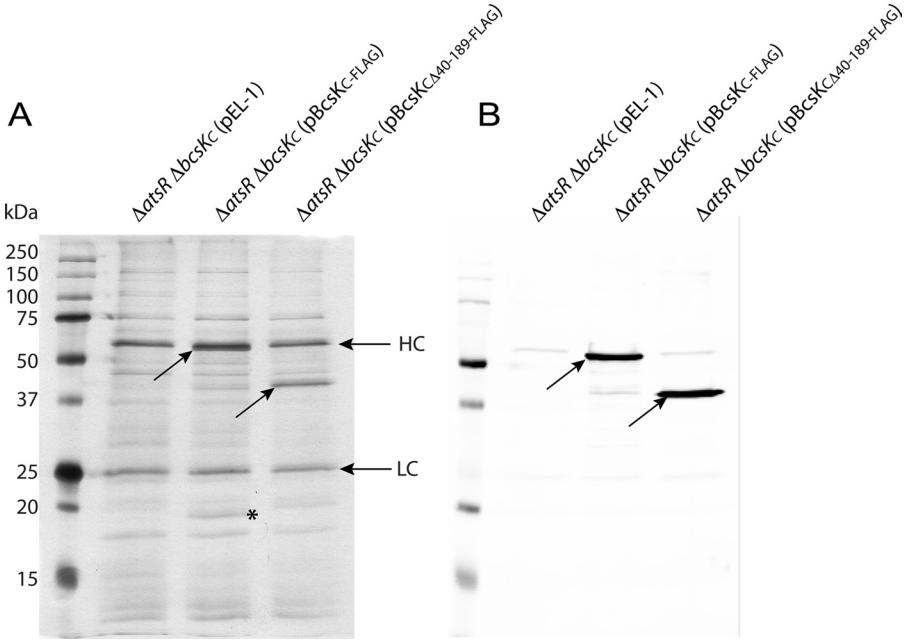

FIGURE 2. **BcsK$_C$ interacts with BcsL$_B$.** Shown is an immunoprecipitation assay using anti-FLAG coupled protein G-agarose beads and cell lysates from *B. cenocepacia* K56-2 Δ*atsR* Δ*bcsK$_C$* harboring pEL-1 (control), pBcsK$_{C\text{-}FLAG}$, or pBcsK$_{CΔ40-189\text{-}FLAG}$. *A*, silver staining. *B*, anti-FLAG Western blot analysis. The *diagonal arrows* highlight the positions of BcsK$_{C\text{-}FLAG}$ and BcsK$_{CΔ40-189\text{-}FLAG}$, whereas the *asterisk* indicates the position of the copurified 20-kDa protein, BcsL$_B$. Protein bands of ~25 and 53 kDa (indicated *LC* and *HC*, respectively) in all samples correspond to the light and heavy chains of the anti-FLAG antibody.

that the N-terminal portion of BcsK$_C$ (amino acids 40–189) is critical for the T6SS activity, suggesting that this region may be required for protein-protein interaction essential for T6SS assembly/stability, correct localization of the protein within the cell, or the intrinsic function of the protein.

BcsK$_C$ Interacts with BcsL$_B$, and the N Terminus of BcsK$_C$ Is Required for the Interaction—Studies in *V. cholerae* and *F. novicida* show that BcsK$_C$ homologs interact with a small T6SS protein homologous to BcsL$_B$ from *B. cenocepacia* (32, 45). To investigate whether BcsK$_C$ also interacts with BcsL$_B$ or with other proteins, we performed pulldown assays using cell lysates from *B. cenocepacia* K56-2 Δ*atsR* Δ*bcsK$_C$* (pEL-1), K56-2 Δ*atsR* Δ*bcsK$_C$* (pBcsK$_{C\text{-}FLAG}$), and K56-2 Δ*atsR* Δ*bcsK$_C$* (pBcsK$_{CΔ40-189\text{-}FLAG}$). As shown in Fig. 2*A*, an additional protein with an apparent mass of ~20 kDa was copurified with BcsK$_{C\text{-}FLAG}$ but not with BcsK$_{CΔ40-189\text{-}FLAG}$, suggesting that the N-terminal portion of BcsK$_C$ is required to bind the 20-kDa protein. Mass spectrometry was performed on the 20-kDa polypeptide and on the corresponding region in lane K56-2 Δ*atsR* Δ*bcsK$_C$* (pBcsK$_{CΔ40-189\text{-}FLAG}$) as control. Mass spectra were searched against the NCBI database with the MASCOT search engine. Identified peptides from the 20-kDa protein matched with good confidence BcsL$_B$ (BCAL0341; 19.2 kDa) with a total protein score of 467 and were absent in the control lane K56-2 Δ*atsR* Δ*bcsK$_C$* (pBcsK$_{CΔ40-189\text{-}FLAG}$).

Bacterial two-hybrid experiments confirmed the BcsK$_C$/BcsL$_B$ interaction. BcsL$_B$ was used as bait and fused to the T25 domain of the adenylate cyclase from *B. pertussis* (pT25BcsL$_B$). BcsK$_C$ and BcsK$_{CΔ40-189}$ were used as prey and fused either to the N terminus of the adenylate cyclase T18 domain using the pUT18 plasmid (pBcsK$_C$T18 and pBcsK$_{CΔ40-189}$T18) or to the C terminus of the T18 domain using the pUT18C plasmid (pT18BcsK$_C$ and pT18BcsK$_{CΔ40-189}$). *E. coli* KEM5 (adenylate cyclase-deficient) harboring pT25BcsL$_B$ was cotransformed with the recombinant plasmids expressing BcsK$_C$ hybrid proteins. Bacterial cultures were spotted on a X-gal containing agar plate, and transcriptional activation of the *lac* operon indicative of protein interaction was visualized by the formation of blue colonies (Fig. 3*A*). The extent of interaction was also estimated by measuring the β-galactosidase activity (Fig. 3*B*). *E. coli* KEM5 colonies harboring pT25BcsL$_B$ together with the vectors pUT18 or pUT18C remained white, indicating that BcsL$_B$ fused to the T25 domain does not interact with the T18 domain alone expressed from

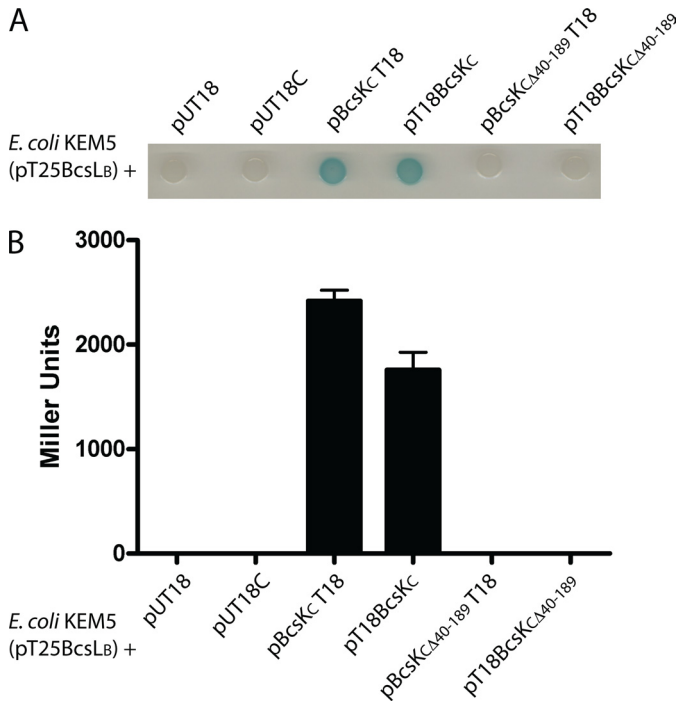

FIGURE 3. **The N terminus of BcsK$_C$ is required for interaction with BcsL$_B$.** *A*, protein interaction using the bacterial two-hybrid system. *E. coli* harboring pT25BcsL$_B$ was cotransformed with pUT18 and pUT18C control vectors or with the recombinant plasmids expressing BcsK$_C$ or BcsK$_{C\Delta 40-189}$ hybrid proteins fused to the T18 domain in pUT18 (pT18BcsK$_C$ and pT18BcsK$_{C\Delta 40-189}$) and in pUT18C (pBcsK$_C$T18 and pBcsK$_{C\Delta 40-189}$T18). Bacterial cultures were spotted on a X-gal containing agar plate and transcriptional activation of the *lac* operon indicative of protein interaction was visualized by the formation of blue colonies. *B*, quantification of the β-galactosidase activity of *E. coli* harboring pT25BcsL$_B$ cotransformed with pUT18, pUT18C, pBcsK$_C$T18, pT18BcsK$_C$, pBcsK$_{C\Delta 40-189}$T18, and pT18BcsK$_{C\Delta 40-189}$. The enzyme activities are expressed in Miller units. The data shown are the means of three independent experiments done in triplicate. The *error bars* represent the standard deviation.

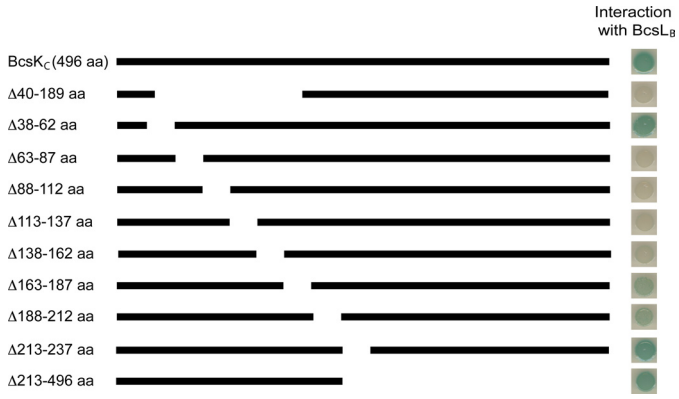

FIGURE 4. **Identification of BcsK$_C$ domains required for interaction with BcsL$_B$.** Protein interaction using the bacterial two-hybrid system. *E. coli* harboring pT25BcsL$_B$ was cotransformed with recombinant plasmids expressing sequentially truncated BcsK$_C$ hybrid proteins fused to the T18 domain in pUT18. Bacterial cultures were spotted on a X-gal containing agar plate, and transcriptional activation of the *lac* operon indicative of protein interaction was visualized by the formation of blue colonies.

pUT18 or pUT18C plasmids. In contrast, *E. coli* KEM5 (pT25BcsL$_B$ + pBcsK$_C$T18) and *E. coli* KEM5 (pT25BcsL$_B$ + pT18BcsK$_C$) formed blue colonies, denoting interacting hybrid proteins and thus confirming that BcsK$_C$ interacts with BcsL$_B$. However, *E. coli* KEM5 (pT25BcsL$_B$ + pBcsK$_{C\Delta 40-189}$T18) and *E. coli* KEM5 (pT25BcsL$_B$ + pT18BcsK$_{C\Delta 40-189}$) formed white colonies, clearly demonstrating that BcsK$_{C\Delta 40-189}$ does not interact with BcsL$_B$ and indicating that the N terminus of BcsK$_C$ is critical for interaction with BcsL$_B$. These results were validated with β-galactosidase assays, thus confirming the interaction between full-length BcsK$_C$ and BcsL$_B$ and the critical role of the BcsK$_C$ N terminus in the interaction (Fig. 3*B*).

To determine the minimal amino acid sequence of BcsK$_C$ required for BcsL$_B$ binding, we constructed a panel of sequential deletions of *bcsK$_C$* (Fig. 4). Truncated BcsK$_C$ proteins were fused to the adenylate cyclase T18 domain and tested for interaction with T25BcsL$_B$. Physical interactions between the hybrid proteins were detected on X-gal-containing plates. Among the deletions tested, only BcsK$_{C\Delta 38-62}$T18, BcsK$_{C\Delta 163-187}$T18, BcsK$_{C\Delta 188-212}$T18, BcsK$_{C\Delta 213-237}$T18, and BcsK$_{C\Delta 213-496}$T18 could bind T25BcsL$_B$ and thus activate the *lacZ* reporter gene (Fig. 4). Interactions between BcsK$_C$T18, BcsK$_{C\Delta 38-62}$T18, BcsK$_{C\Delta 213-237}$T18, and BcsK$_{C\Delta 213-496}$T18 and T25BcsL$_B$ were detected on the plate after only 24 h of incubation at 30 °C (data not shown). By contrast, interactions between either BcsK$_{C\Delta 163-187}$T18-T25BcsL$_B$ or BcsK$_{C\Delta 188-212}$T18-T25BcsL$_B$ required 48 h of incubation, indicating that BcsK$_{C\Delta 163-187}$T18 and BcsK$_{C\Delta 188-212}$T18 interact weakly with T25BcsL$_B$. After 1 week of incubation, BcsK$_{C\Delta 113-137}$T18 and BcsK$_{C\Delta 138-162}$T18 eventually turned blue, whereas BcsK$_{C\Delta 63-87}$T18 and BcsK$_{C\Delta 88-112}$T18 remained unable to activate *lacZ* (data not shown). Together, these results suggest that the N terminus of BcsK$_C$ (amino acids 2–212) is sufficient for the interaction with BcsL$_B$. Within the BcsK$_C$ N-terminal domain, amino acids 88–162 are important for BcsK$_C$/BcsL$_B$ interaction, and more precisely the region encompassing amino acid 63–112 is essential for interaction with BcsL$_B$.

BcsK$_C$ Is Tightly Associated with the Outer Membrane—BcsK$_C$ lacks a signal peptide sequence as predicted by the SignalP 3.0 program (54, 55), and *in silico* analysis of the BcsK$_C$ protein using different transmembrane helices prediction programs available at the ExPASY Proteomics and PSIPRED servers (46, 47) was not conclusive. BcsK$_C$ is predicted to have either no transmembrane domain (DAS, SOSUI, and TMHMM) or one transmembrane domain (HMMTOP, TMpred, TopPred, MEMSAT) whose position and orientation differ depending on the algorithm used (supplemental Fig. S2).

Cell fractionations were performed to determine the subcellular localization of BcsK$_{C\text{-}FLAG}$ and its truncated derivative BcsK$_{C\Delta 40-189\text{-}FLAG}$. As shown in Fig. 5*A*, BcsK$_{C\text{-}FLAG}$ and BcsK$_{C\Delta 40-189\text{-}FLAG}$ proteins localized both in the soluble fraction and the membrane fraction, suggesting that deletion of the N terminus of BcsK$_C$ does not affect the protein localization. The membrane fraction containing BcsK$_{C\text{-}FLAG}$ was incubated with various reagents (Fig. 5*B*). BcsK$_{C\text{-}FLAG}$ was not released with high salt (1 M NaCl) but was partially solubilized by 6 M urea and nonionic detergent (3% Triton X-100). BcsK$_{C\text{-}FLAG}$ was completely solubilized by strong ionic detergents (1% SDS) and 2% *N*-lauroylsarcosine, which solubilizes both inner and outer membrane under the conditions tested (supplemental Fig. S3). Together, these data suggest that BcsK$_C$ is a tightly associated to the bacterial membrane. The membrane localiza-

tion of BcsK$_C$ was further investigated by using sucrose density gradients to separate the inner from the outer membrane. As shown in Fig. 5*C*, BcsK$_{C\text{-FLAG}}$ did not cofractionate with the NADH oxidase activity but with BCAM1931, an outer membrane porin from *B. cenocepacia*, indicating that BcsK$_{C\text{-FLAG}}$ is associated with the outer membrane.

BcsK$_C$ Forms a High Molecular Weight Complex Containing BcsL$_B$ and Also Requiring BcsF$_H$ for Its Formation—Expression of BcsK$_{C\text{-FLAG}}$ in *B. cenocepacia* K56-2 Δ*atsR* Δ*bcsK$_C$* leads to the formation of a high molecular weight complex detected with the anti-FLAG antibody at the top of the separating gel (Fig. 5*A*, *lane 3*), suggesting multimerization of BcsK$_{C\text{-FLAG}}$. This complex localizes almost exclusively in the membrane fraction (Fig. 5*A*, *lanes 2* and *3*) and is anchored to the outer membrane (Fig. 5*C*). The complex was absent when BcsK$_{C\Delta 40-189\text{-FLAG}}$ was expressed in K56-2 Δ*atsR* Δ*bcsK$_C$*, suggesting that the N terminus of BcsK$_C$ is required for the complex formation (Fig. 5*A*, *lanes 3* and *6*). Moreover, although a complex is formed when BcsK$_{C\text{-FLAG}}$ is expressed in *B. cenocepacia* K56-2 Δ*atsR* Δ*bcsK$_C$*, expression of BcsK$_{C\text{-FLAG}}$ in a strain where all the T6SS encoding genes have been deleted (K56-2 Δ*atsR* Δ*T6SS*) did not allow the complex formation, indicating that other T6SS components are required (Fig. 5*A*, *lanes 3*, *6*, and *9*).

We investigated which T6SS components were required for the formation of the BcsK$_{C\text{-FLAG}}$-containing complex. In *B. cenocepacia* K56-2 the T6SS gene cluster is organized in three putative transcriptional units (Fig. 6*A*). To identify the components involved in the BcsK$_C$-containing complex formation, each of the three transcriptional units were individually deleted in the K56-2 Δ*atsR* (K56-2 Δ*atsR* Δ*TU1*, K56-2 Δ*atsR* Δ*TU2*, and K56-2 Δ*atsR* Δ*TU3*). The cell lysates were prepared from the different mutant strains expressing

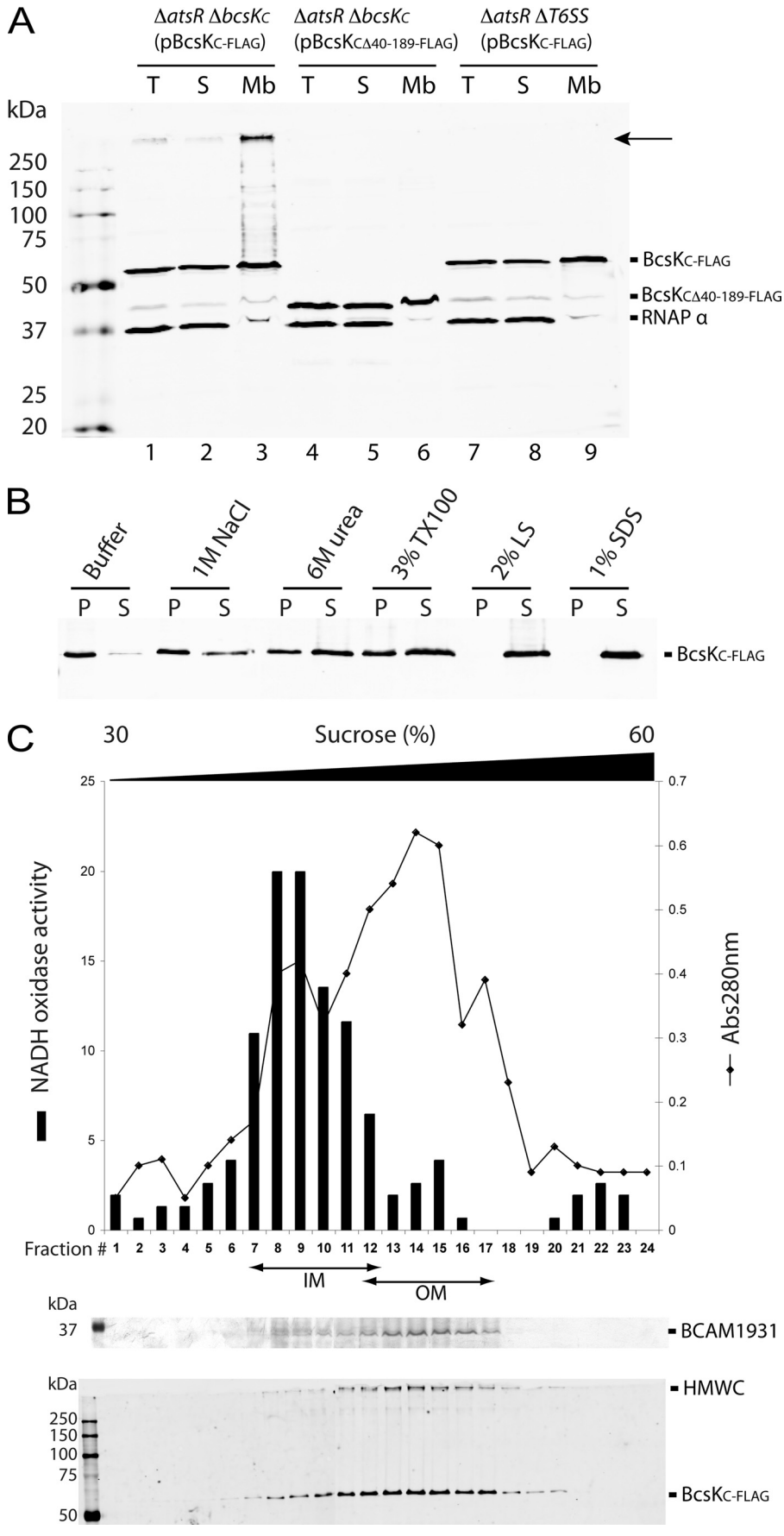

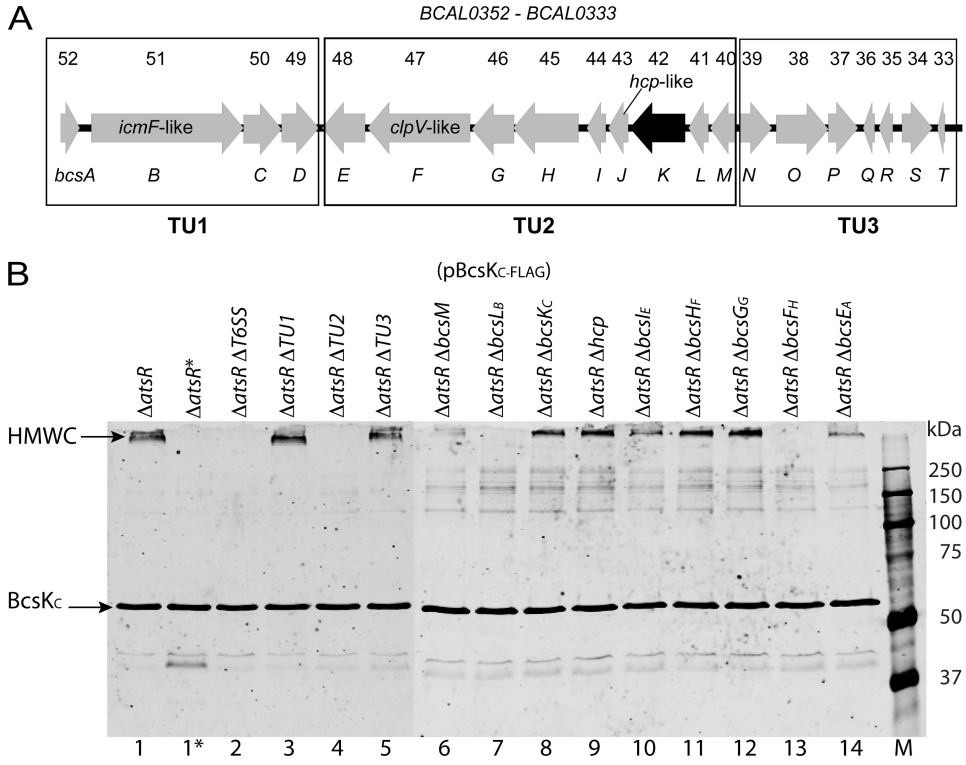

FIGURE 6. **BcsL$_B$ and BcsF$_H$ are required for the formation of the BcsK$_C$-containing high molecular mass complex.** *A*, genetic map of the T6SS gene cluster. This cluster has been designated *bcs* cluster for *B. cenocepacia* survival. The *arrows* represent the location and direction of gene transcription. *BCAL* gene designations according to the annotation of the *B. cenocepacia* J2315 genome (53) are shown above, and the *bcs* annotation of the genes is shown below. The genes *icmF-like* (*BCAL0351*, *bcsB$_M$*), *clpV-like* (*BCAL0347*, *bcsF$_H$*), and *hcp$_{Bc}$* (*BCAL0343*, *bcsJ$_D$*), which are hallmarks of T6SSs in other bacteria, are shown. The *black arrow* represents *bcsK$_C$*. The putative transcriptional units TU1, TU2, and TU3 are *boxed*. *B*, anti-FLAG Western blot analysis of total cell lysates recovered from *B. cenocepacia* K56-2 mutant strains harboring pBcsK$_{C\text{-}FLAG}$. *Lane 1*, K56-2 Δ*atsR*; *lane 2*, K56-2 Δ*atsR* Δ*T6SS*; *lane 3*, K56-2 Δ*atsR* Δ*TU1*; *lane 4*, K56-2 Δ*atsR* Δ*TU2*; *lane 5*, K56-2 Δ*atsR* Δ*TU3*; *lane 6*, K56-2 Δ*atsR* Δ*bcsM*; *lane 7*, K56-2 Δ*atsR* Δ*bcsL$_B$*; *lane 8*, K56-2 Δ*atsR* Δ*bcsK$_C$*; *lane 9*, K56-2 Δ*atsR* Δ*hcp*; *lane 10*, K56-2 Δ*atsR* Δ*bcsI$_E$*; *lane 11*, K56-2 Δ*atsR* Δ*bcsH$_F$*; *lane 12*, K56-2 Δ*atsR* Δ*bcsG$_G$*; *lane 13*, K56-2 Δ*atsR* Δ*bcsF$_H$*; *lane 14*, K56-2 Δ*atsR* Δ*bcsE$_A$*; *lane M*, molecular mass markers with the indicated sizes (kDa). The *asterisk* indicates that the sample has been boiled prior to loading. *Black arrows* indicate BcsK$_C$ or the high molecular mass complex (*HMWC*).

BcsK$_{C\text{-}FLAG}$ and analyzed by Western blot. As shown Fig. 6*B*, strains K56-2 Δ*atsR* Δ*TU1* (pBcsK$_{C\text{-}FLAG}$) (*lane 3*) and K56-2 Δ*atsR* Δ*TU3* (pBcsK$_{C\text{-}FLAG}$) (*lane 5*) but not K56-2 Δ*atsR* Δ*TU2* (pBcsK$_{C\text{-}FLAG}$) (*lane 4*) could produce the BcsK$_C$-containing complex, suggesting that the TU2 contains the critical components for complex formation. Each gene of the TU2 was systematically deleted in K56-2 Δ*atsR* (Fig. 6*A*). Cell lysate analysis of individual gene mutants within the TU2 revealed that BcsL$_B$ and BcsF$_H$ were required for the formation of the BcsK$_{C\text{-}FLAG}$-containing complex (Fig. 6*B*, *lanes 7* and *13*).

The complex is heat-sensitive because it was not detectable in samples that were heated prior to loading (Fig. 6*B*, *lane 1**). To investigate the composition of the complex unheated membrane, samples prepared from K56-2 Δ*atsR* Δ*bcsK$_C$* (pBcsK$_{C\text{-}FLAG}$) and K56-2 Δ*atsR* Δ*T6SS* (pBcsK$_{C\text{-}FLAG}$) were individually run on a SDS-PAGE gel. A slice from the top of the separating gels containing high molecular weight proteins (and the BcsK$_C$-containing complex in the case of K56-2 Δ*atsR* Δ*bcsK$_C$* (pBcsK$_{C\text{-}FLAG}$)) was excised. The proteins were electroeluted and concentrated, and the samples were heated prior to loading on a SDS-PAGE gel to disassociate the components of the BcsK$_C$-containing complex. Comparison of the protein profiles of K56-2 Δ*atsR* Δ*bcsK$_C$* (pBcsK$_{C\text{-}FLAG}$) and K56-2 Δ*atsR* Δ*T6SS* (pBcsK$_{C\text{-}FLAG}$) revealed two extra bands in the electroeluted sample from K56-2 Δ*atsR* Δ*bcsK$_C$* (pBcsK$_{C\text{-}FLAG}$) with apparent masses of ~55 and ~20 kDa (Fig. 7). Mass spectrometry was performed on those two proteins. Identified peptides matched with a score of 507 and 643 to BCAL0342 (BcsK$_C$) and BCAL0341 (BcsL$_B$), respectively, indicating that BcsL$_B$ is also part of the complex containing BcsK$_C$ and again confirms the interaction between BcsK$_C$ and BcsL$_B$.

DISCUSSION

In this study, we show that deletion of *bcsK$_C$* abolishes T6SS-associated phenotypes in *B. cenocepacia* (Hcp secretion and induction of the cytoskeletal rearrangements in macrophages after infection), demonstrating that BcsK$_C$ is a key component of the *B. cenocepacia* T6SS. Most T6SSs identified to date encode a BcsK$_C$ homolog, and the importance of BcsK$_C$-like proteins in T6SS activity has already been underlined in other Gram-negative bacteria such as

FIGURE 5. **BcsK$_C$ is tightly associated with the outer membrane.** *A*, Western blot analysis of total cell lysate (*T*), soluble (*S*), and total membrane (*Mb*) fractions recovered from *B. cenocepacia* K56-2 Δ*atsR* Δ*bcsK$_C$* (pBcsK$_{C\text{-}FLAG}$), K56-2 Δ*atsR* Δ*bcsK$_C$* (pBcsK$_{CΔ40-189\text{-}FLAG}$), and *B. cenocepacia* K56-2 Δ*atsR* Δ*T6SS* (pBcsK$_{C\text{-}FLAG}$) using anti-FLAG and anti-RNAP α subunit antibodies (cytosolic control). Ten μg of protein were loaded on a 12% SDS-PAGE gel. Molecular mass marker sizes (kDa) are shown on the *left*. The *arrow* highlights the position of the BcsK$_{C\text{-}FLAG}$-containing complex. The faint bands seen in the membrane fractions (*lines 3*, *6*, and *9*) at the RNAP α subunit location (~37 kDa) correspond to an unspecific protein cross-reacting with the anti-FLAG antibody (see Fig. 6*B*). *B*, protein solubilization. Total membranes were incubated with 50 mM Tris-HCl, pH 7.4 (*Buffer*), 1 M NaCl, 3% Triton X-100 (*TX100*), 2% *N*-lauroylsarcosine (*LS*), or 1% SDS. Insoluble (pellet, *P*) and soluble (supernatant, *S*) fractions were loaded on a 12% SDS-PAGE gel and analyzed by Western blot using an anti-FLAG antibody. *C*, sucrose density gradient. Inner and outer membranes were separated on a discontinuous sucrose gradient. The protein content was calculated by measuring the $A_{280\ nm}$, and the quality of the fractionation was assessed by measuring the enzymatic activity of the NADH oxidase (inner membrane marker) and by detecting the porin BCAM1931 (outer membrane marker). Fractions 1–24 were loaded on 12% SDS-PAGE gels and silver-stained or analyzed using an anti-FLAG antibody. The position of BCAM1931, BcsK$_{C\text{-}FLAG}$ and the high molecular mass complex (*HMWC*) are indicated. The positions of the inner membrane-containing (*IM*) and outer membrane-containing (*OM*) fractions are indicated.

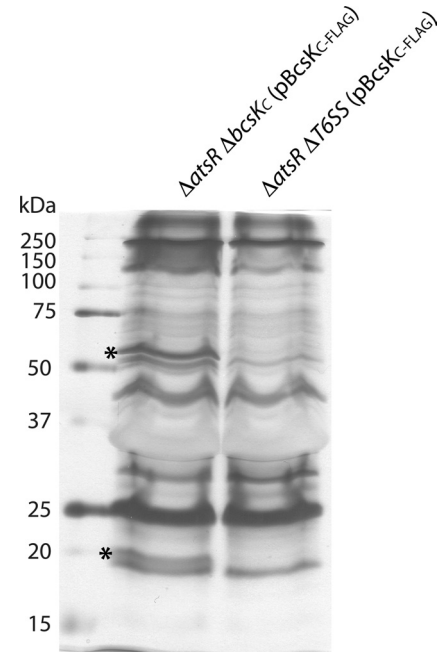

FIGURE 7. **The high molecular mass complex contains BcsK$_C$ and BcsL$_B$.** Seventy μg of electroeluted high molecular mass proteins recovered from *B. cenocepacia* K56-2 Δ*atsR* Δ*bcsK$_C$* (pBcsK$_{C\text{-}FLAG}$) (*left lane*) and K56-2 Δ*atsR* Δ*T6SS* (pBcsK$_{C\text{-}FLAG}$) (*right lane*) were boiled and loaded on a 16% SDS-PAGE gel. The *asterisks* highlight the positions of the 55- and 20-kDa proteins subjected to mass spectrometry analysis and corresponding to BcsK$_C$ and BcsL$_B$, respectively. Shown at *left* are the molecular weight markers with the indicated sizes (kDa).

enteroaggregative *E. coli*, *E. tarda*, and *F. novicida* (11, 12, 14). In *B. mallei*, the BcsK$_C$ homolog TssB (BMAA0743) is not required for Hcp secretion, but it is necessary for virulence in hamsters (22). *B. mallei* contains three paralogs sharing more than 30% homology with TssB amino acid sequence. Redundancy might explain why Hcp is still secreted but does not explain the lack of virulence when TssB is mutated. Schell *et al.* (22) speculated that TssB is a secreted effector instead of a component of the T6S apparatus, but this remains to be demonstrated.

We also demonstrated that BcsK$_C$ could interact with BcsL$_B$ as shown by our immunoprecipitation and bacterial two-hybrid assays. This was an expected result because interactions between proteins homologous to BcsK$_C$ and BcsL$_B$ have already been reported in other T6S systems (11, 32, 45). For example, in *F. novicida*, the central region of IglA (BcsL$_B$ homolog) is required for interaction with IglB (BcsK$_C$ homolog) (45). Using a similar approach, our study reveals that the region required to bind BcsL$_B$ is limited to the N terminus of BcsK$_C$, in particular to a segment encompassing amino acids 63–112. The N terminus of BcsK$_C$, likely because of its ability to bind BcsL$_B$, is essential for T6SS activity. PSIPRED analysis predicted this region to form two α helices preceding a β strand. *Ab initio* structural modeling of BcsK$_C$, VipB, IglB, and PA0084 using the I-Tasser server (48) revealed a similar fold in the regions corresponding to amino acids 63–112 of BcsK$_C$, which consists of paired α-helices (supplemental Fig. S4). Therefore, we propose that this is a conserved domain among BcsK$_C$-like proteins for the interaction with BcsL$_B$-like proteins.

Using a purified protein fusion containing the N terminus of ClpV and soluble cell lysate from *V. cholerae* Bönemann *et al.* (32) demonstrated that the N terminus of ClpV interacts with the VipA/VipB complex (BcsL$_B$/BcsK$_C$ homolog). Interaction between BcsF$_H$ (ClpV homolog) and BcsK$_C$/BcsL$_B$ has not been detected in our pulldown assays or our electroelution/resolution of the BcsK$_C$-containing complex under the conditions tested. In *V. cholerae* ClpV is eight times less abundant than VipA and VipB (32). Thus, if the same ratio is true for *B. cenocepacia*, ClpV and BcsL$_B$/BcsK$_C$ interactions might be more difficult to detect when BcsK$_C$ is used as bait in immunoprecipitation assays. Moreover, because the energizing component ClpV has been shown in *V. cholerae* to degrade BcsL$_B$/BcsK$_C$-like cytosolic complexes, it is possible that ClpV interacts with BcsL$_B$/BcsK$_C$ transiently. Interaction between IglA/IglB in *F. novicida* has been shown to be required for the stability of each protein (45). In our experimental conditions BcsK$_C$ and derivatives are constitutively expressed on a multi-copy plasmid at higher levels than it would be in the wild type strain. Constitutive expression of BcsK$_{C\Delta 40-189\text{-}FLAG}$ (unable to bind BcsL$_B$) in *B. cenocepacia* K56-2 Δ*atsR* or of BcsK$_{C\text{-}FLAG}$ in a *B. cenocepacia* K56-2 Δ*atsR* Δ*bcsL$_B$* background likely bypassed the protein stability issue because no reduction of the protein expression levels or degradation products were noticed in the different cell lysates.

BcsL$_B$ and BcsK$_C$ homologs have been proposed to have different cellular localizations. In *V. cholerae*, the BcsL$_B$ and BcsK$_C$ homologs VipA and VipB have been described as non-secreted cytosolic proteins (32). In *F. novicida*, the BcsL$_B$ and BcsK$_C$ homologs IglA and IglB have been described as strictly cytosolic proteins (11) or as surface-exposed proteins (49, 50). In *E. tarda*, EvpA (BcsL$_B$) interacts with the periplasmic domain of IcmF (12), suggesting that BcsL$_B$ homologs might have a periplasmic location. By using a different approach and constitutively expressing BcsK$_C$ on a plasmid in *B. cenocepacia* K56-2 Δ*atsR* (overexpressing the other T6SS components), we show that BcsK$_C$ can be found in the cytosol but also in strong association with the outer membrane. In our fractionation analysis we noticed that BcsK$_C$ forms a high molecular weight complex anchored to the outer membrane. The formation of this complex depends on two other T6SS encoded proteins, BcsL$_B$ and BcsF$_H$ (ClpV homolog). Purification and analysis of the complex composition showed that BcsL$_B$ is also part of the complex (Fig. 7). The high molecular weight complex containing BcsK$_C$ and BcsL$_B$ may be indicative of the Type VI secretion structure; however, no other proteins could be detected as part of the complex under the conditions tested. If any other proteins are part of the complex, their amount is likely below the level of detection of our technique. In *V. cholerae*, BcsL$_B$ and BcsK$_C$ homologs VipA and VipB form cytosolic tubules disassembled by ClpV (32). However, in contrast to VipA/VipB tubules, the *B. cenocepacia* BcsL$_B$/BcsK$_C$ complex was consistently detected in the membrane fraction, but not in the soluble fraction containing the cytosolic proteins. Furthermore, the BcsL$_B$/BcsK$_C$ complex requires ClpV for its formation, whereas in *V. cholerae* the VipA/VipB tubule-like structures are severed by ClpV (32). Together, these data

suggest that even though the BcsL$_B$/BcsK$_C$ complex and the VipA/VipB tubules are made of BcsK$_C$/BcsL$_B$-like proteins, they have different localizations and likely reflect different stages in the biogenesis of the T6S apparatus. Leiman *et al.* (21) found that the characteristics of this VipA/B structure resemble those of the contracted T4 phage tail sheath (51) and speculated that VipA/B may provide energy to the T6SS-mediated secretion and membrane insertion process through conformational changes that mimic those that occur during phage tail contraction. Because of the similarities between the architectures of the VipA/VipB tubules and the bacteriophage T4 tail sheath, Bönemann *et al.* (52) proposed recently that VipA/VipB tubules might represent structural core components of the T6SS and that biogenesis of T6SSs might require ClpV to export VipA and VipB subunits into the periplasm, followed by VipA/VipB tubule reformation. We propose that the BcsL$_B$/BcsK$_C$ complex that we describe in this study reflects precisely the tubule formation in the periplasmic space, which would be anchored to the outer membrane. Further characterization of BcsK$_C$/BcsL$_B$-like complexes is needed to understand their role in the functioning of the T6SS.

Acknowledgments—We thank Dr. M. Soledad Saldías and Slade Loutet for critical review of the manuscript, and Danuta Radzioch (McGill University, Department of Human Genetics, Montreal General Hospital Research Institute, Montreal, Canada) for the gift of the ANA-1 cell line.

REFERENCES

1. Vanlaere, E., Baldwin, A., Gevers, D., Henry, D., De Brandt, E., LiPuma, J. J., Mahenthiralingam, E., Speert, D. P., Dowson, C., and Vandamme, P. (2009) *Int. J. Syst. Evol. Microbiol.* **59,** 102–111
2. Vanlaere, E., Lipuma, J. J., Baldwin, A., Henry, D., De Brandt, E., Mahenthiralingam, E., Speert, D., Dowson, C., and Vandamme, P. (2008) *Int. J. Syst. Evol. Microbiol.* **58,** 1580–1590
3. Govan, J. R., and Deretic, V. (1996) *Microbiol. Rev.* **60,** 539–574
4. Reik, R., Spilker, T., and Lipuma, J. J. (2005) *J. Clin. Microbiol.* **43,** 2926–2928
5. Speert, D. P., Henry, D., Vandamme, P., Corey, M., and Mahenthiralingam, E. (2002) *Emerg. Infect. Dis.* **8,** 181–187
6. Mahenthiralingam, E., Vandamme, P., Campbell, M. E., Henry, D. A., Gravelle, A. M., Wong, L. T., Davidson, A. G., Wilcox, P. G., Nakielna, B., and Speert, D. P. (2001) *Clin. Infect. Dis.* **33,** 1469–1475
7. Hunt, T. A., Kooi, C., Sokol, P. A., and Valvano, M. A. (2004) *Infect. Immun.* **72,** 4010–4022
8. Aubert, D. F., Flannagan, R. S., and Valvano, M. A. (2008) *Infect. Immun.* **76,** 1979–1991
9. Das, S., and Chaudhuri, K. (2003) *In Silico Biol.* **3,** 287–300
10. Rao, P. S., Yamada, Y., Tan, Y. P., and Leung, K. Y. (2004) *Mol. Microbiol.* **53,** 573–586
11. de Bruin, O. M., Ludu, J. S., and Nano, F. E. (2007) *BMC Microbiol.* **7,** 1
12. Zheng, J., and Leung, K. Y. (2007) *Mol. Microbiol.* **66,** 1192–1206
13. Pukatzki, S., Ma, A. T., Revel, A. T., Sturtevant, D., and Mekalanos, J. J. (2007) *Proc. Natl. Acad. Sci. U.S.A.* **104,** 15508–15513
14. Dudley, E. G., Thomson, N. R., Parkhill, J., Morin, N. P., and Nataro, J. P. (2006) *Mol. Microbiol.* **61,** 1267–1282
15. Bladergroen, M. R., Badelt, K., and Spaink, H. P. (2003) *Mol. Plant Microbe Interact.* **16,** 53–64
16. Pukatzki, S., Ma, A. T., Sturtevant, D., Krastins, B., Sarracino, D., Nelson, W. C., Heidelberg, J. F., and Mekalanos, J. J. (2006) *Proc. Natl. Acad. Sci. U.S.A.* **103,** 1528–1533
17. Mougous, J. D., Cuff, M. E., Raunser, S., Shen, A., Zhou, M., Gifford, C. A., Goodman, A. L., Joachimiak, G., Ordoñez, C. L., Lory, S., Walz, T., Joachimiak, A., and Mekalanos, J. J. (2006) *Science* **312,** 1526–1530
18. Wu, H. Y., Chung, P. C., Shih, H. W., Wen, S. R., and Lai, E. M. (2008) *J. Bacteriol.* **190,** 2841–2850
19. Ishikawa, T., Rompikuntal, P. K., Lindmark, B., Milton, D. L., and Wai, S. N. (2009) *PLoS One* **4,** e6734
20. Filloux, A., Hachani, A., and Bleves, S. (2008) *Microbiology* **154,** 1570–1583
21. Leiman, P. G., Basler, M., Ramagopal, U. A., Bonanno, J. B., Sauder, J. M., Pukatzki, S., Burley, S. K., Almo, S. C., and Mekalanos, J. J. (2009) *Proc. Natl. Acad. Sci. U.S.A.* **106,** 4154–4159
22. Schell, M. A., Ulrich, R. L., Ribot, W. J., Brueggemann, E. E., Hines, H. B., Chen, D., Lipscomb, L., Kim, H. S., Mrázek, J., Nierman, W. C., and Deshazer, D. (2007) *Mol. Microbiol.* **64,** 1466–1485
23. Suarez, G., Sierra, J. C., Sha, J., Wang, S., Erova, T. E., Fadl, A. A., Foltz, S. M., Horneman, A. J., and Chopra, A. K. (2008) *Microb. Pathog.* (2008) **44,** 344–361
24. Ma, A. T., McAuley, S., Pukatzki, S., and Mekalanos, J. J. (2009) *Cell Host Microbe* **5,** 234–243
25. Hood, R. D., Singh, P., Hsu, F., Güvener, T., Carl, M. A., Trinidad, R. R., Silverman, J. M., Ohlson, B. B., Hicks, K. G., Plemel, R. L., Li, M., Schwarz, S., Wang, W. Y., Merz, A. J., Goodlett, D. R., and Mougous, J. D. (2010) *Cell Host Microbe* **7,** 25–37
26. Khajanchi, B. K., Sha, J., Kozlova, E. V., Erova, T. E., Suarez, G., Sierra, J. C., Popov, V. L., Horneman, A. J., and Chopra, A. K. (2009) *Microbiology* **155,** 3518–3531
27. Parsons, D. A., and Heffron, F. (2005) *Infect. Immun.* **73,** 4338–4345
28. Pell, L. G., Kanelis, V., Donaldson, L. W., Howell, P. L., and Davidson, A. R. (2009) *Proc. Natl. Acad. Sci. U.S.A.* **106,** 4160–4165
29. Ma, L. S., Lin, J. S., and Lai, E. M. (2009) *J. Bacteriol.* **191,** 4316–4329
30. Aschtgen, M. S., Bernard, C. S., De Bentzmann, S., Lloubès, R., and Cascales, E. (2008) *J. Bacteriol.* **190,** 7523–7531
31. Aschtgen, M. S., Gavioli, M., Dessen, A., Lloubes, R., and Cascales, E. (2001) *Mol. Microbiol.* **75,** 886–899
32. Bönemann, G., Pietrosiuk, A., Diemand, A., Zentgraf, H., and Mogk, A. (2009) *EMBO J.* **28,** 315–325
33. Cascales, E. (2008) *EMBO Rep.* **9,** 735–741
34. Shalom, G., Shaw, J. G., and Thomas, M. S. (2007) *Microbiology* **153,** 2689–2699
35. Sambrook, J., Fritsch, E. F., and Maniatis, T. (1989) *Molecular Cloning: A Laboratory Manual*, 2nd Ed., Cold Spring Harbor Laboratory, Cold Spring Harbor, NY
36. Cohen, S. N., Chang, A. C., and Hsu, L. (1972) *Proc. Natl. Acad. Sci. U.S.A.* **69,** 2110–2114
37. Figurski, D. H., and Helinski, D. R. (1979) *Proc. Natl. Acad. Sci. U.S.A.* **76,** 1648–1652
38. Craig, F. F., Coote, J. G., Parton, R., Freer, J. H., and Gilmour, N. J. (1989) *J. Gen. Microbiol.* **135,** 2885–2890
39. Flannagan, R. S., Linn, T., and Valvano, M. A. (2008) *Environ. Microbiol.* **10,** 1652–1660
40. Blum, H., Beier, H., and Gross, H. J. (1987) *Electrophoresis* **8,** 93–99
41. Karimova, G., Pidoux, J., Ullmann, A., and Ladant, D. (1998) *Proc. Natl. Acad. Sci. U.S.A.* **95,** 5752–5756
42. Putnam, S. L., and Koch, A. L. (1975) *Anal. Biochem.* **63,** 350–360
43. Osborn, M. J., Gander, J. E., Parisi, E., and Carson, J. (1972) *J. Biol. Chem.* **247,** 3962–3972
44. Cox, G. W., Mathieson, B. J., Gandino, L., Blasi, E., Radzioch, D., and Varesio, L. (1989) *J. Natl. Cancer Inst.* **81,** 1492–1496
45. Bröms, J. E., Lavander, M., and Sjöstedt, A. (2009) *J. Bacteriol.* **191,** 2431–2446
46. Jones, D. T. (1999) *J. Mol. Biol.* **292,** 195–202
47. McGuffin, L. J., Bryson, K., and Jones, D. T. (2000) *Bioinformatics* **16,** 404–405
48. Zhang, Y. (2008) *BMC Bioinformatics* **9,** 40
49. Melillo, A., Sledjeski, D. D., Lipski, S., Wooten, R. M., Basrur, V., and Lafontaine, E. R. (2006) *FEMS Microbiol. Lett.* **263,** 102–108
50. Ludu, J. S., de Bruin, O. M., Duplantis, B. N., Schmerk, C. L., Chou, A. Y., Elkins, K. L., and Nano, F. E. (2008) *J. Bacteriol.* **190,** 4584–4595

51. Moody, M. F. (1967) *J. Mol. Biol.* **25,** 167–200
52. Bönemann, G., Pietrosiuk, A., and Mogk, A. (2010) *Mol Microbiol* **76,** 815–821
53. Holden, M. T., Seth-Smith, H. M., Crossman, L. C., Sebaihia, M., Bentley, S. D., Cerdeño-Tárraga, A. M., Thomson, N. R., Bason, N., Quail, M. A., Sharp, S., Cherevach, I., Churcher, C., Goodhead, I., Hauser, H., Holroyd, N., Mungall, K., Scott, P., Walker, D., White, B., Rose, H., Iversen, P., Mil-Homens, D., Rocha, E. P., Fialho, A. M., Baldwin, A., Dowson, C., Barrell, B. G., Govan, J. R., Vandamme, P., Hart, C. A., Mahenthiralingam, E., and Parkhill, J. (2009) *J. Bacteriol.* **191,** 261–277
54. Nielsen, H., Engelbrecht, J., Brunak, S., and von Heijne, G. (1997) *Protein Eng.* **10,** 1–6
55. Bendtsen, J. D., Nielsen, H., von Heijne, G., and Brunak, S. (2004) *J. Mol. Biol.* **340,** 783–795